Hydrogen Balmer line broadening in Ar-N2-SiH4 DC glow discharge.

Jean-Louis Jauberteau, Isabelle Jauberteau

Hydrogen Balmer line broadening in Ar-N_2-SiH_4 DC glow discharge.

J. L. Jauberteau, I. Jauberteau

Université de Limoges, UMR 7315 CNRS, SPCTS, 12 rue Atlantis, 87068 Limoges, France

Electronic mail for correspondence: jean-louis.jauberteau@unilim.fr

Abstract.

Broadened hydrogen Balmer lines are observed in a DC glow discharge sustained in Ar-SiH_4-N_2 gas mixture. This broadening is due to the Doppler frequency shift. H atoms translational energy distribution is calculated in different positions between the two electrodes of the discharge along the inter electrode axis and in different gas mixtures. Three main components are observed at 0.6 (+/-0.5)eV, 12(+/-3)eV, 62(+/-6)eV and 1(+/-1)eV, 28(+/-6)eV and 105(+/-12)eV for Hα and Hβ, respectively. They correspond to hydrogen dissociation by electron impact producing H(n=3, 4) atoms and to dissociative recombination of ion in the cathode fall or to back-scattered fast H atoms on the cathode surface. The density ratio nH_2/nAr ranges from 44% to 13% or from 10% to 3% when a=nH/nH_2=0.01 and 0.1, respectively, in function of the gas mixture. So large hydrogen density could be due to hydrogen desorption from the wall and cathodes and/or to the gas recirculation within the reactor. A new low energy component is observed in Hα line profile, when silane and nitrogen concentration decreases and increases, respectively. It could also be due to H atom desorbing from the reactor wall or to NH_x species dissociated by electron impact within the reactor.

Keywords: Ar-SiH_4-N_2 plasma, Hydrogen Balmer emission line broadening, Doppler effect, reactive processes, hydrogen concentration.

I. INTRODUCTION

Plasma enhanced chemical vapour deposition are widely used for surface treatments and silane or disilane are frequently used for silicon nitride or silicon oxide thin films deposition for surface passivation or to elaborate dielectric layers.[1-3] The knowledge of the basic phenomena involved in the growth of these layers is very important to control the process and to obtain stable and reproducible thin films. Reactive mechanisms involved in these discharges are generally complex and are produce both within the discharge (homogeneous reactions) and at the surface layer (heterogeneous reactions).[4-6] Investigations on reactive

species produced in such discharge are generally performed by means of optical spectroscopy, [3,5] Langmuir probe or mass spectrometry.[7-8]

During the past few decades authors have reported on Doppler broadening of Balmer lines observed by means of optical emission spectroscopy in silane, disilane, methane or hydrogen discharge.[9-17] They have shown that the broadening mainly results from the dissociation processes due to electron impacts on molecules, producing super excited repulsive states or to the acceleration of ions in the cathode fall before to be neutralised.

The purpose of this work is to study hydrogen Balmer lines broadening, observed in a DC glow discharge sustained in Ar-SiH_4-N_2 gas mixture, to determine the main reactive processes producing excited hydrogen atoms with high velocity. We will see that this broadening can be due to the combination of different effects.

II. EXPERIMENTAL SETUP

The experimental setup is schematically shown on Figure1. A DC discharge is created between two aluminium flat electrodes (inter electrode distance=17mm and electrode diameter=70mm) within a cylindrical observation chamber (diameter 400mm and height 400mm), equipped with fused silica window (diameter 50mm) protected against deposition by a controlled argon flow.

High purity grade gases (99.9955%) are used: pure argon, nitrogen and Argon-5%silane gas mixture. Gas flow rates are controlled and measured by means of mass flowmeters (Tylan) and the absolute pressure is measured by a capacitive manometer (MKS-Baratron). The gas mixture (N_2, Ar-5%SiH_4) is injected within the discharge through the upper electrode (anode). Under working conditions the current intensity, discharge voltage and total pressure are equal to 13mA, 400V and 0.53mbar, respectively. Spatially resolved spectroscopy is performed between the two electrodes, perpendicularly to the inter electrode axis, using a high resolution spectrometer (Jobin Yvon THR1000, resolving power 100000, 1m focal length), equipped with a photomultiplier Hamamatsu R928. The spatial resolution according to the z longitudinal axis of the discharge is obtained by means of an optical setting composed with two multi dielectric mirrors (M1, M2), lenses with a focal of 200mm (L1, L2) and collimators (C1, C2), as shown on figure 1. The upper part of the optical setting (C1, L1, M1) can be moved according to the z axis. The discharge is imaged with of magnification of unity and reflected by the mirror M1 then M2 toward the entrance slit of the spectrometer (aperture of 25µm to 30µm). A spatial resolution of about 1mm is obtained depending on the entrance slit and collimators apertures. Under these experimental conditions, no self absorption is

considered for the different emission lines detected and because of the reactor configuration the discharge is assumed uniform according to the radial axis.

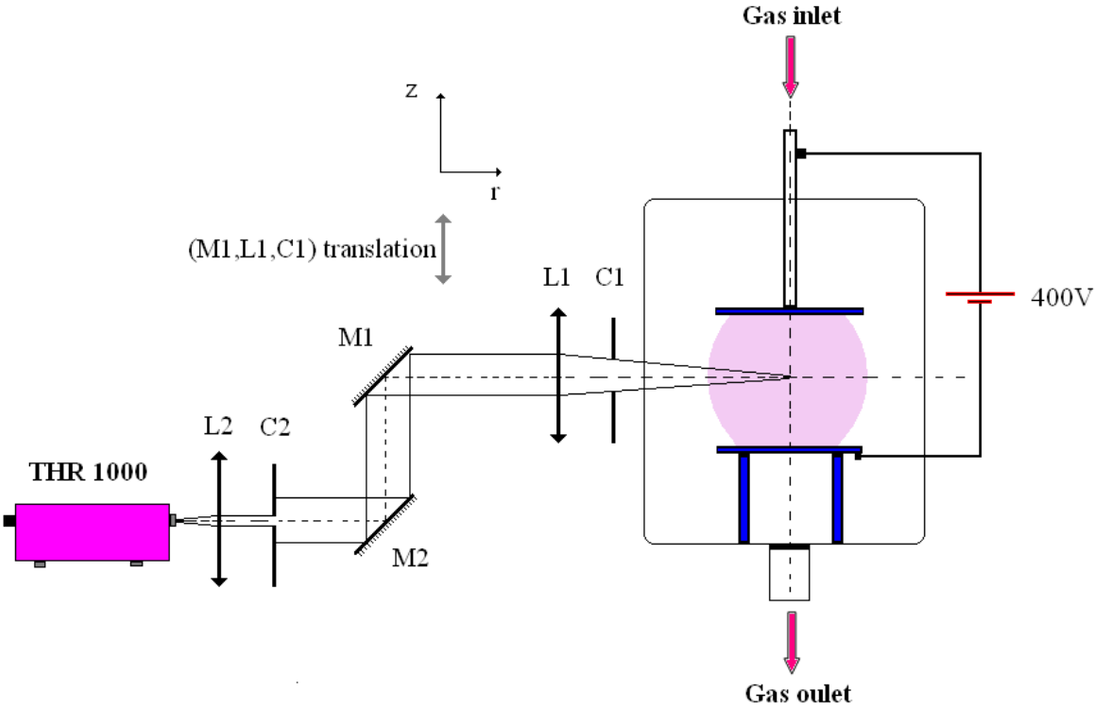

FIG.1. *Experimental setup.*

III. RESULTS AND DISCUSSION

Emission spectroscopy measurements spatially resolved have been performed along the discharge axis at different distances ranging from 2mm to 10mm from the cathode surface. Investigations have been performed on the two hydrogen Balmer lines Hα (656.3nm) and Hβ (486.1nm). A large broadening has been observed for these two emission lines. Figure 2 compare typical emission lines: Hα, Hβ and ArII(413.1nm). The full width at half the maximum (FWHM) are 3.5Å and 3.0Å for Hα and Hβ, and 0.5Å for ArII, respectively.

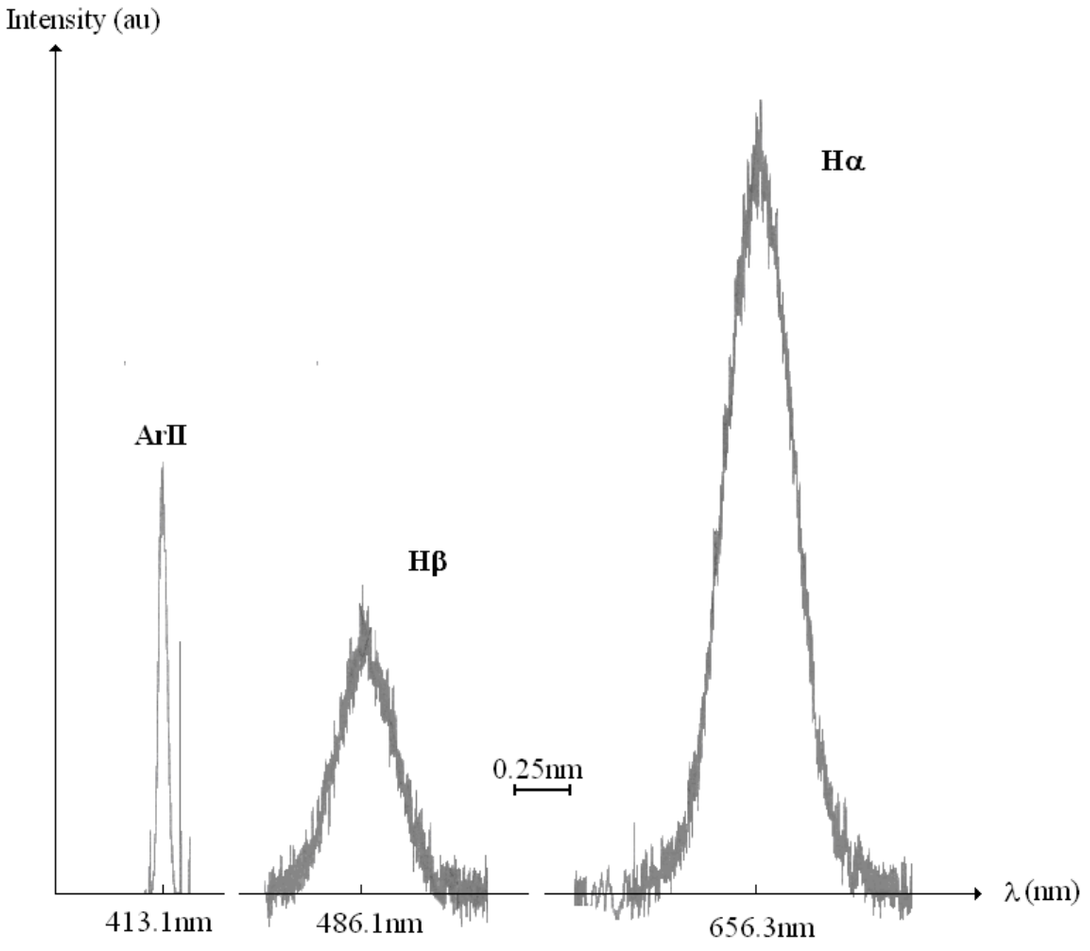

FIG.2. *Emission lines measured for ArII(413.1nm), Hα (656.3nm) and Hβ (486.1nm); Comparison of the emission line widths.*

Since Stark effect starts to be efficient in the discharge medium when the electron density is larger than $10^{18}m^{-3}$, because of the low electron density observed in such DC discharge working under such experimental conditions (typically of $10^{15}m^{-3}$),[15] the broadening results mainly of the Doppler effect. This is confirmed on Figure 3 where Hα line profile can be fitted with a Gaussian profile $I(\lambda) = 9.6\exp\left(-22.86\Delta\lambda^2\right)$ and not with a Lorentzian profile $I(\lambda) = \frac{\Gamma}{2\pi}\frac{1}{\left[\frac{\Gamma^2}{4}+\Delta\lambda^2\right]}$ (where Γ is the FWHM), rather used for the Stark effect.[18] We will see that this Gaussian profile results of the convolution of different components.

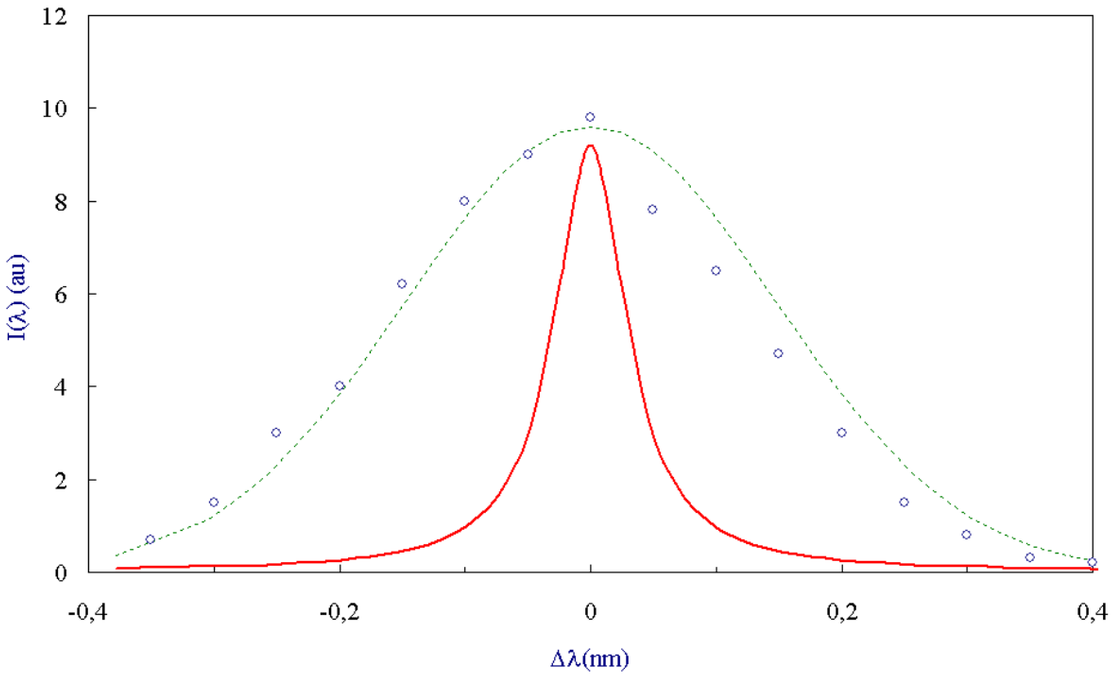

FIG.3. *The Hα line obtained in Ar-5%SiH₄ at 0.53mbar and at 6mm from the cathode. Comparison of experiment (dots) with the best fit obtained with a Gaussian profile (dashed line)* $I(\lambda) = 9.6\exp\left(-22.86\Delta\lambda^2\right)$ *and a Lorentzian profile (full line).*

Figure 4 shows the change of the Hα line profile in different positions from the cathode along the discharge axis. Measurements have been performed for different gas mixtures and at constant total gas flow rate 20sccm and at 0.53mbar. It can be seen that the peak intensity changes between the two electrodes in Ar-5%SiH_4 (see first spectrum at the top of the figure). The maximum is observed at 6mm from the cathode. This position corresponds to the end of the negative glow and the beginning of the positive column of the discharge. The same effect is observed on the Hβ line profile.

When N_2 is added to the gas mixture, the intensity of the wings (larger parts) of Hα line profile strongly decreases with Ar-SiH_4 flow rate decreasing and a new thin component appears at the middle of the line corresponding to slow hydrogen atoms. This component decreases when the nitrogen gas flow rate becomes larger than 5sccm.

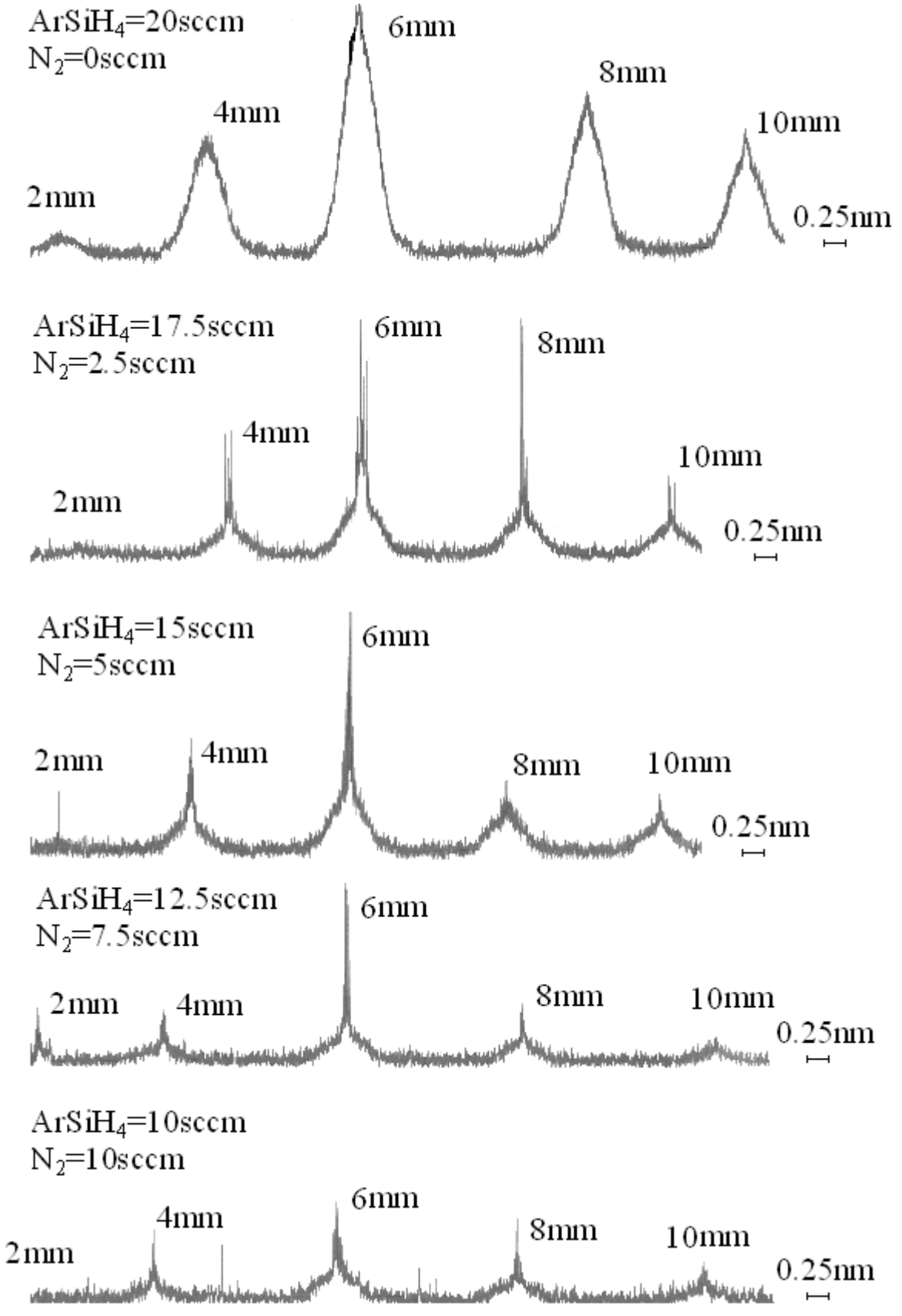

FIG.4. *Comparison of the Hα Balmer line measured in different positions from 2mm to 10mm above the cathode along the discharge axis and for different gas mixtures, the total gas flow rate is of 20sccm and the total pressure of 0.53mbar.*

Because the optical observations are performed perpendicularly to the discharge axis, assuming an isotropic velocity distribution function, the translational energy distribution T(λ) of the hydrogen atoms in the n=3 and n=4 excited states may be calculated by differentiation of the Hα and Hβ line profiles F(λ),[13]

$$T(\lambda) = \frac{-d\left(F(\lambda)\right)}{d\lambda} \quad . \qquad (1)$$

The kinetic energy E of the emitter at the wavelength λ is given by,

$$E = \frac{1}{2} m_H c^2 \left(\frac{\lambda - \lambda_0}{\lambda_0} \right)^2 . \qquad (2)$$

Where m_H is the hydrogen atom mass, c is the light velocity and λ_0 is the wavelength at the center of the emission line. The change from the broadening Δλ(nm) in translational energy E(eV) is obtained using the equations $E(eV) = 1084.75(\Delta\lambda(nm))^2$ and $E(eV) = 1976.9(\Delta\lambda(nm))^2$ for Hα and Hβ, respectively.

Figure 5 shows the translational energy distribution T(λ), measured for Hα and Hβ in the N_2(2.3sccm), (Ar-5%SiH_4)(20sccm) gas mixture. Measurements are performed perpendicularly to the discharge axis.

Different components are observed at 0.023nm, 0.107nm, 0.24nm and 0.023m, 0.107nm, 0.23nm for Hα and Hβ, respectively. They are found at energy of 0.6 (+/-0.5)eV, 12(+/-3)eV, 62(+/-6)eV and 1(+/-1)eV, 28(+/-6)eV and 105(+/-12)eV for Hα and Hβ, respectively. The error bars are calculated assuming an error of 0.01nm on Δ(λ). According to literature, such peaks have been observed in Ar-SiH_4 and Ar-H_2 plasma.

Perrin et al[13] have observed different peaks on Hβ at 0.4eV, 2.5eV and a broad component in the 3-6eV region in Ar-SiH_4 multipole DC discharge. These peaks appear at different electron impact energy use for the dissociation of the silane molecule, ranging from 27eV to 110eV.

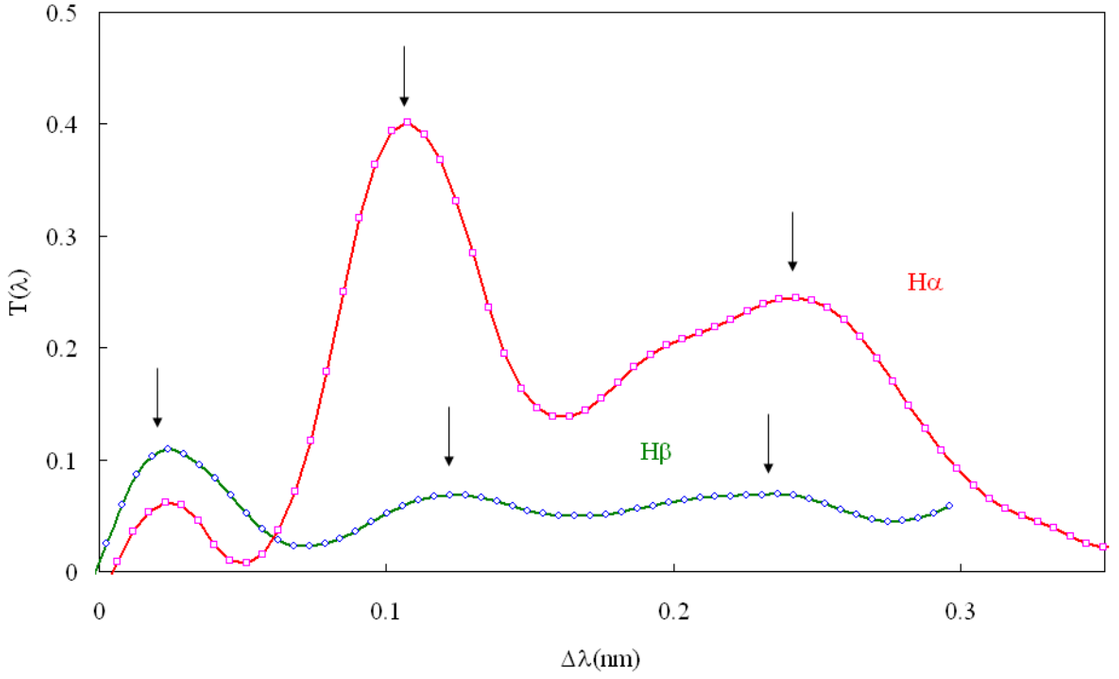

FIG.5. *Translational energy distribution T(λ), measured for Hα and Hβ in a N_2(2.3sccm), Ar-5%SiH_4(20sccm) gas mixture. Measurements are performed perpendicularly to the discharge axis.*

Different mechanisms in Ar-H_2 gas mixture can produce H atoms in excited states. They are: [9-12, 14-17]

1) The dissociation of H_2 by electron impact with excitation of H(n=3). Two components have been observed at 0.2eV and at higher energy about 7.5eV.

2) The dissociative ionisation of H_2 by electron impact, this reaction can also produce H(n=3) with a kinetic energy around 5.5eV and 8eV. The electron energy needs for this reaction is more important that for the previous one and consequently it is less probable to occur.

3) H(n=3) may be formed also by electron impact on H(1s) atom, resulting of previous dissociation reactions. In this process two components are found for H atoms, one below 2eV and a medium at energy between 5eV and 10eV.

4) Barbeau et al[15] observe a very large shift, up to 0.5nm, of Hα in a plane parallel DC discharge sustained in a Ar-H_2 gas mixture. The wavelength shift depends on the region of observation perpendicular to the discharge axis and it increases with decreasing distance from the cathode surface. They conclude that the electric field in the cathode fall has an effect on the Doppler shift and that a so large shift could be due to ion recombination in the cathode fall.

Gemišić Adamov et al,[11] observe very large broadenings on Hα and Dα with a Doppler shift up to 1KeV in an abnormal glow discharge sustained in Ar-H_2 gas mixture. Most of hydrogen or deuterium atoms have energy around 40-50eV. Because H atom energy cannot exceed 10eV in dissociative excitation process due to electron impacts on H_2 molecules, such broadened wings have been ascribed to charge-exchange reaction between hydrogen ions (H^+, H_2^+, H_3^+) accelerated in the cathode fall region and H_2 molecules. These fast ions, atoms or molecules are back-scattered from the cathode in the form of fast H atoms which are finally excited by collision with electrons or H_2.[12]

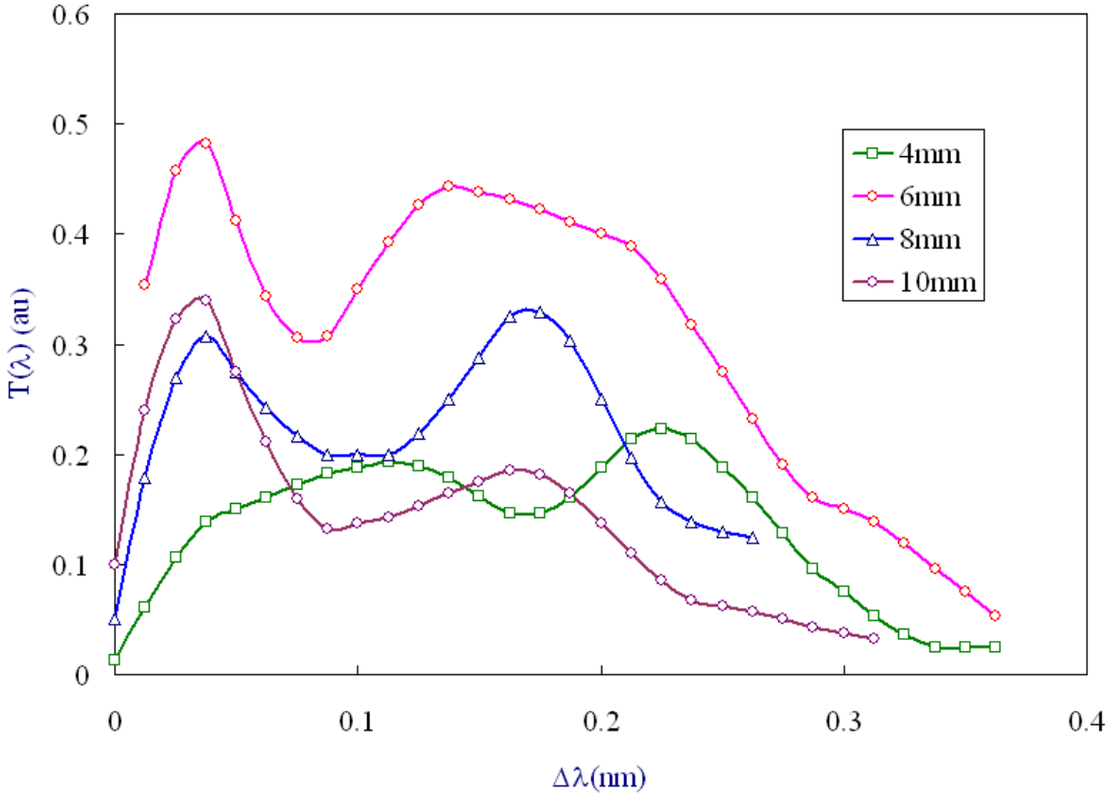

FIG.6. *Translational energy distribution of H atoms measured on Hα in Ar-SiH_4 discharge at 0.53mbar in different positions from the cathode surface. Observations are performed perpendicularly to the inter electrode discharge axis.*

Figure 6 shows the translational energy distribution of H(n=3) measured in different positions from the cathode surface. The three main components previously described figure 5 are observed at 0.037nm, 0.125nm and 0.23nm. In can be seen that the larger components at 0.23nm is mainly observed at a distance close to the cathode surface and it disappears with increasing distance. This confirms the previous observations of Barbeau et al[15] and Gemišić

Adamov et al.[11] The large energy components observed at 62 (+/-6)eV on Hα could be due to the dissociative recombination of ions in the cathode fall or to back-scattered fast H atoms on the cathode surface. At 0.53mbar, the molecular mean free path is about 10^{-4}m and back scattered H atoms have many collisions in the inter electrode distance. So a gradient of the concentration of these fast H atoms can be observed between the two electrodes.

Comparing with our results (figure 5) the two first components are more probably due to the dissociation of H_2 or excitation of H atom than to SiH_4 dissociation processes.

In the next part of this article, we focus our investigations on the Hα profiles; the Hβ lines are smaller and more subject to uncertain results than Hα.

More investigations are necessary to complete the observations on the translational energy distribution and to confirm the previous results. This needs the knowledge of the electron temperature in order to calculate the different collision integrals and to compare the effect of the different reactive processes under consideration.

The electron temperature has been determined from the emission line ratio of neutral and ion argon ArI(419.1nm) and ArII(413.1nm). These emission lines correspond to the transitions between energy levels of 14.58eV to 11.77eV and 21.43eV to 18.43ev of Ar and Ar^+, respectively.[19] Assuming that these excited species are produced by direct excitation due to electron impact on Ar atom in the ground state and writing the intensity $I_i(\lambda)$ of the spectral line,

$$I_i(\lambda) = C(\lambda).n_i A_i h\nu \,. \qquad (3)$$

Where, $C(\lambda)$, n_i, A_i and ν are the apparatus response, the density of the excited state for Ar or Ar^+, the transition probability ($0.0058\text{x}10^8 s^{-1}$ for ArI(419.1nm) and $1.4\text{x}10^8 s^{-1}$ for ArII(413.1nm)[20-22]) and the emission frequency, respectively.

The apparatus responses depends on the quantum efficiency $Q(\lambda)$ of the photomultiplier, on the efficiency of the spectrometer holographic grating and on the change of lenses optical properties (focal, transmission) at the different wavelength λ. The quartz refractive index can be considered constant, changing from 1.45 at 656.3nm to 1.47 at 413.1nm and the quartz transmittance is constant and larger than 90% all over the wavelength range under investigation. Also the efficiency of the spectrometer grating is nearly constant (about 50%) all over the same wavelength range. Consequently, the change of the apparatus responses with the wavelength depends mainly on the quantum efficiency $Q(\lambda)$ of the photomultiplier.

Change of lenses and spectrometer grating optical properties have no significant effect on C(λ) all over the wavelength range under consideration.

Assuming a local thermodynamic equilibrium, the electron energy can be considered to be a Maxwell-Boltzmann distribution function and the electron temperature is deduced from the $I(Ar^+)/I(Ar)$ intensity ratio,

$$\frac{I(Ar^+)}{I(Ar)} = \frac{C(\lambda_{Ar+})}{C(\lambda_{Ar})}\frac{n^*_{Ar+}}{n^*_{Ar}}\frac{A(\lambda_{Ar+})}{A(\lambda_{Ar})}\frac{\nu_{Ar+}}{\nu_{Ar}} = \frac{C(\lambda_{Ar+})}{C(\lambda_{Ar})}\frac{\int_0^\infty \sigma_{Ar+}(\varepsilon_e) f(\varepsilon_e) d\varepsilon_e}{\int_0^\infty \sigma_{Ar}(\varepsilon_e) f(\varepsilon_e) d\varepsilon_e}\frac{A(\lambda_{Ar+})}{A(\lambda_{Ar})}\frac{\lambda_{Ar}}{\lambda_{Ar+}} \qquad (4)$$

Using the excitation cross section values given in literature for ArI(4191.1nm)[23] and for ArII(413.2)nm,[24] we have calculated the value of the ratio $I(Ar^+)/I(Ar)$ using the Equation (4), for different values of the electron temperature Te. These values are compared to the experimental values. Figure 7 shows the experimental values corresponding to two series of data (I and J) obtained at 13mA, 400V and 0.53mbar, in Ar-5%SiH_4 and pure Ar, respectively. Measurements are performed in different positions along the inter electrode distance. The error bar on IAr^+/IAr is 15%. Figure 8 shows the values calculated using the Equation (4) versus electron temperature. It can be seen that the values of measured $I(Ar^+)/I(Ar)$ ratio (figure 7) correspond to an electron temperature of about 30000K ($I(Ar^+)/I(Ar)$= 2.79).

It is worth noting that in this method we suppose that the Ar^+ excited state $\left[4p^2P^0_{1/2}\right]$ results of the direct excitation from the Ar ground state by electron collision and the excitation from the ion ground state is neglected. According to literature, assuming a ionization fraction of $3x10^{-3}$, the contribution of the excitation from the ion ground state contribute for more than half of the total photon flux of ArII(488.0nm) emission line for an electron temperature lower than 7eV.[25] If we consider a similar effect for the ArII(4131.1nm) emission line, the contribution of the excitation of the $\left[4p^2P^0_{1/2}\right]$ state from the ion ground state is half of the total excitation and the ratio $I(Ar^+)/I(Ar)$ in Equation (4) should be divided by 2, ranging from 0.5 to 1.8. Under these conditions the electron temperature ranges from 25000K to 30000K as shown on Figure 8. Moreover, it is worth noting that an ionization fraction of $3x10^{-3}$ is overestimated in the case of a DC glow discharge working at 400V, 13mA and 0.53mbar. In the present experiments the electron density is expected between $10^{15}m^{-3}$ and $10^{17}m^{-3}$ [15] and

the contribution of the excitation from the ion ground state to the ArII (4131.1nm) is also overestimated.

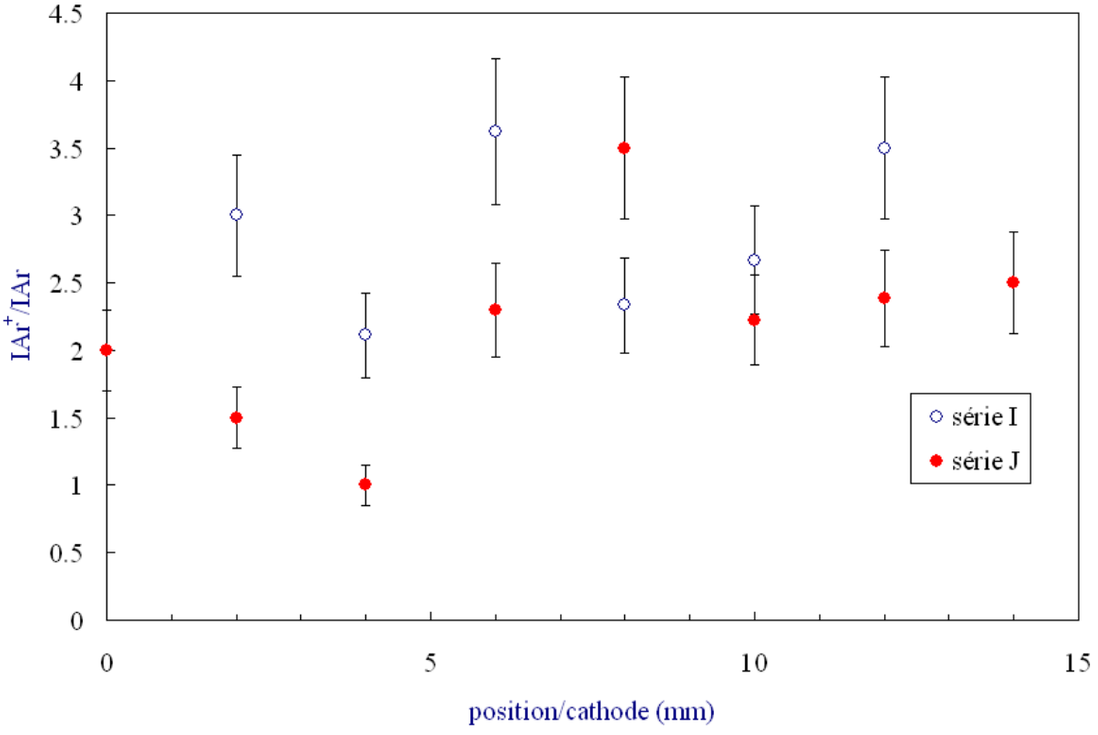

FIG.7. *Relative intensity of IArII(413.1nm)/IArI(419.1nm) versus distance from the cathode along the inter electrode axis in pure argon (series I) and in Ar-%SiH₄ (series J), at 400V, 13mA and 0.53mbar.*

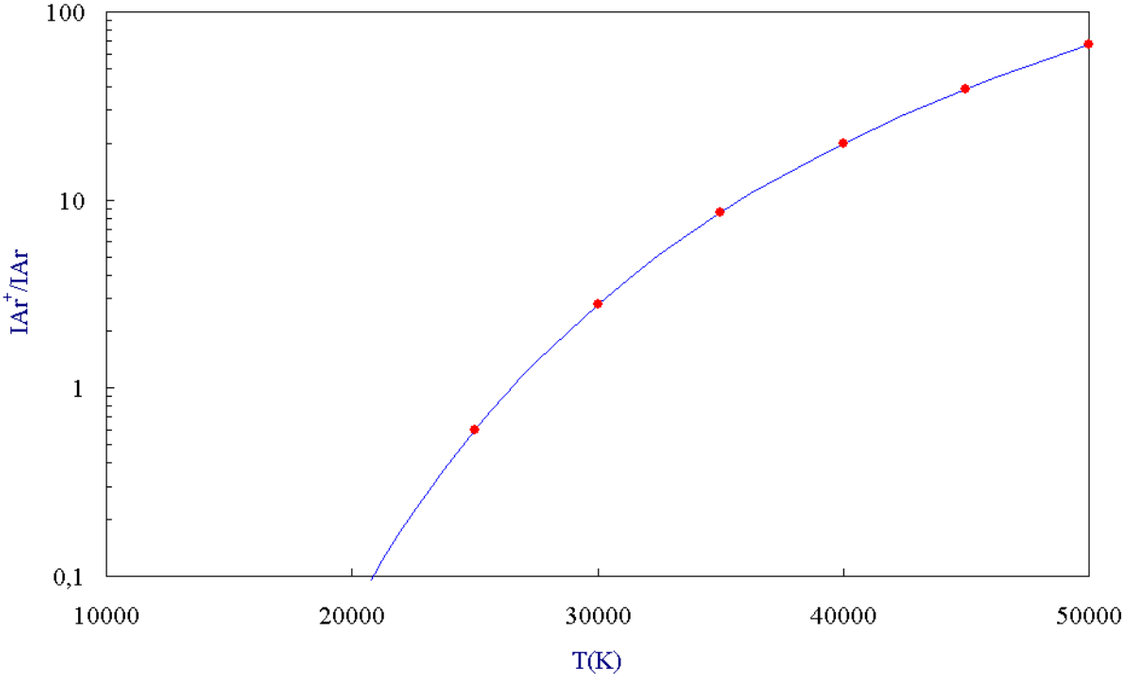

FIG.8. *Calculation of the relative intensity IArII(413.1nm)/IArI(419.1nm) value versus electron temperature.*

As previously explained and according to the literature the different reactive processes which can contribute to the Hα emission line are the dissociative excitation of molecular species, the direct excitation of H by electron collision or the ion dissociative recombination in the cathode fall with the back-scattering of fast H atoms.[9-17] We have already shown that this last process (ion dissociative recombination in the cathode fall and back-scattered fast H atoms) have only an effect on Hα line close to the cathode. For measurements performed at larger distances from the cathode the main mechanisms which can produce H(n=3) atoms are:

The dissociative excitation of SiH_4 by electron impact:

$e+SiH_4 \rightarrow e+H(n=3)+products$ [reaction I]

The dissociative excitation of H_2 by electron impact:

$e+H_2 \rightarrow e+H(n=3)+H$ [reaction II]

The direct excitation of H:

$e+H \rightarrow e+H(n=3)$ [reaction III].

The total intensity of Hα is the sum of three components corresponding to these different mechanisms,

$$IH\alpha = IH(1) + IH(2) + IH(3)$$

Using Equation (3), the intensity of Hα is,

$$I_{H\alpha} = \sum_i I_{H(i)} = C(\lambda) A_{H\alpha} \frac{hc}{\lambda} \sum_i n_{H(i)} \qquad (5)$$

With i=1,2 or3, according to the process under consideration ([reaction I, II or III].

Comparing the emission line measured for Hα and Ar(419.1nm), we have also,

$$\frac{I_{H\alpha}}{I_{Ar}} = \frac{C(\lambda_{H\alpha})}{C(\lambda_{Ar})} \frac{n_{H^*}}{n_{Ar^*}} \frac{\lambda_{Ar}}{\lambda_{H\alpha}} \frac{A_{H\alpha}}{A_{Ar}} \qquad (6)$$

So,

$$\frac{n_{H^*}}{n_{Ar^*}} = \frac{I_{H\alpha}}{I_{Ar}} \frac{Q(\lambda_{Ar})}{Q(\lambda_{H\alpha})} \frac{\lambda_{H\alpha}}{\lambda_{Ar}} \frac{A_{Ar}}{A_{H\alpha}} = f(\frac{I_{H\alpha}}{I_{Ar}}), \qquad (7)$$

where $f(I_{H\alpha}/I_{Ar})$ is a function depending on the ratio $I_{H\alpha}/I_{Ar}$ and on the quantum efficiency of the photomultiplier tube $Q(\lambda_{H\alpha})=7\%$ and $Q(\lambda_{Ar})=20\%$ at the two wavelengths $\lambda_{H\alpha}=656.2$nm and $\lambda_{Ar}=419.1$nm, respectively and on the transition probability of the two excited species $A_{H\alpha}=0.441\text{x}10^8\text{s}^{-1}$ and $A_{Ar}=0.0056\text{x}10^8\text{s}^{-1}$.

Considering that Ar* results of direct electron collisions on Ar ground state and considering $n_{H(i=1)}$ due to process (1), we have

$$\frac{n_{H^*(i=1)}}{n_{Ar^*}} = \frac{n_e n_{siH4} \int_0^\infty \sigma_{SiH4} f(\varepsilon_e) d\varepsilon_e}{n_e n_{Ar} \int_0^\infty \sigma_{Ar} f(\varepsilon_e) d\varepsilon_e} = \frac{n_{siH4}}{n_{Ar}} \frac{\int_0^\infty \sigma_{SiH4} f(\varepsilon_e) d\varepsilon_e}{\int_0^\infty \sigma_{Ar} f(\varepsilon_e) d\varepsilon_e} \qquad (8)$$

Using Equations (7) and (8) we obtain the relative contribution of process (1) to the total emission line of Hα,

$$\frac{n_{H^*(i=1)}}{n_{H^*}} = \frac{n_{H^*(i=1)} \big/ n_{Ar^*}}{n_{H^*} \big/ n_{Ar^*}} = \frac{n_{SiH4}}{n_{Ar}} \frac{\int_0^\infty \sigma_{SiH4} f(\varepsilon_e) d\varepsilon_e}{\int_0^\infty \sigma_{Ar} f(\varepsilon_e) d\varepsilon_e} \frac{1}{f(\frac{I_{H\alpha}}{I_{Ar}})} \qquad (9)$$

From Equation (9), considering Te=30000K and the dissociation cross section values given in [26] for the dissociative excitation of silane by electron impact, we have calculated the ratio $\frac{n_{H^*(i=1)}}{n_{H^*}}$ in different (Ar-5%SiH_4)-N_2 gas mixtures, at 13mA and 400V, with $D_{Ar\text{-}SiH4}=20$sccm and D_{N2} ranging from 0sccm to 10.2sccm. Integrating the signal over the total Hα emission line, we obtain $\frac{n_{H^*(i=1)}}{n_{H^*}}$ ranging from 0.01 to 0.03 (see Figure 9). This result shows the low contribution of SiH_4 dissociation process to the total density of H(n=3) (lower than 4%).

Writing the density ratio $\frac{n_H}{n_{H_2}} = a$ and neglecting the low contribution of the first process (1) to the total excitation of H(n=3), we have,

$$\frac{\sum_i n_{H(i)^*}}{n_{H^*}} \approx \frac{n_{H(i=2)} + n_{H(i=3)}}{n_{H^*}} = \frac{n_{H2} \big/ n_{Ar}}{f(\frac{I_{H\alpha}}{I_{Ar}})} \left\{ \frac{\int_0^\infty \sigma_{H2} f(\varepsilon_e) d\varepsilon_e}{\int_0^\infty \sigma_{Ar} f(\varepsilon_e) d\varepsilon_e} + a \frac{\int_0^\infty \sigma_H f(\varepsilon_e) d\varepsilon_e}{\int_0^\infty \sigma_{Ar} f(\varepsilon_e) d\varepsilon_e} \right\} = 1 \qquad (10)$$

Then,

$$\frac{n_{H2}}{n_{Ar}} = f(\frac{I_{H\alpha}}{I_{Ar}}) \frac{1}{\left\{ \frac{\int_0^\infty \sigma_{H2} f(\varepsilon_e) d\varepsilon_e}{\int_0^\infty \sigma_{Ar} f(\varepsilon_e) d\varepsilon_e} + a \frac{\int_0^\infty \sigma_{H} f(\varepsilon_e) d\varepsilon_e}{\int_0^\infty \sigma_{Ar} f(\varepsilon_e) d\varepsilon_e} \right\}} . \quad (11)$$

It can be seen that when the part due to the mechanism 1 is neglected, the contribution of the mechanism (2) to the total excitation of H(n=3), only depends on the collision integral of mechanisms 1 and 2 and on the value a. Using Equations (7) and (11), we obtain,

$$\frac{n_{H^*(i=2)}}{n_{H^*}} = \frac{n_{H^*(i=2)} / n_{Ar^*}}{n_{H^*} / n_{Ar^*}} = \frac{n_{H_2}}{n_{Ar}} \frac{\int_0^\infty \sigma_{H_2} f(\varepsilon_e) d\varepsilon_e}{\int_0^\infty \sigma_{Ar} f(\varepsilon_e) d\varepsilon_e} \frac{1}{f(\frac{I_{H\alpha}}{I_{Ar}})} = \left(1 + a \frac{\int_0^\infty \sigma_{H} f(\varepsilon_e) d\varepsilon_e}{\int_0^\infty \sigma_{H_2} f(\varepsilon_e) d\varepsilon_e} \right)^{-1} . \quad (12)$$

Calculations have been performed using data given by H. Tawara et al [27] and by .K. Janev et al [28] for the cross section values of the photon emission of Balmer α line due to the electron impact on H_2 and H atoms, respectively.

Figure 9 also shows the ratio $\frac{n_{H_2}}{n_{Ar}}$ which decreases with N_2 increasing from DN_2=2.3sccm to DN_2=10.2sccm, when DAr-SiH_4 is kept constant equal to 20sccm. The ratio strongly depends on the "a" value. It changes versus DN_2 from 44% to 14%, and from 10% to 3% for a=0.01 and a=0.1, respectively. When a=0.01 about 64% of Hα emission line results of the H_2 dissociation process (2). However, when a=0.1 and a=0.5, Hα only depends at 15% and 3.5% on mechanism (2), respectively. Nevertheless, for a<0.4 the contribution due to the mechanism (2) remains larger than the contribution due to the mechanism (1).

According to literature, in H_2 DC discharge the dissociation rate of hydrogen is about 10% for pressure ranging from 0.07mbar to 0.75mbar, at 600K, voltage ranging from 0.5kV to 3kV and intensity ranging from 6mA to 39mA.[15] In our experiment, the atom or molecular mean free path is about 10^{-4}m, thus H atoms quickly recombine. So the ratio $\frac{n_H}{n_{H_2}} = a$ is expected to be between 0.01 and 0.1. Considering the low concentration of silane in Argon (5%), such a large density value of H_2 until a=0.1, which is mainly observed at low nitrogen gas flow rate, could be explained considering the wall desorption and the recirculation of H_2 within the reactor.[29-30] In the past, authors have already observed that H_2 partial pressure may exceed the

silane partial pressure in Silane-Helium glow discharge, even when the dominant reactive dissociation process of silane by electron impact produces SiH_2+H_2.[31]

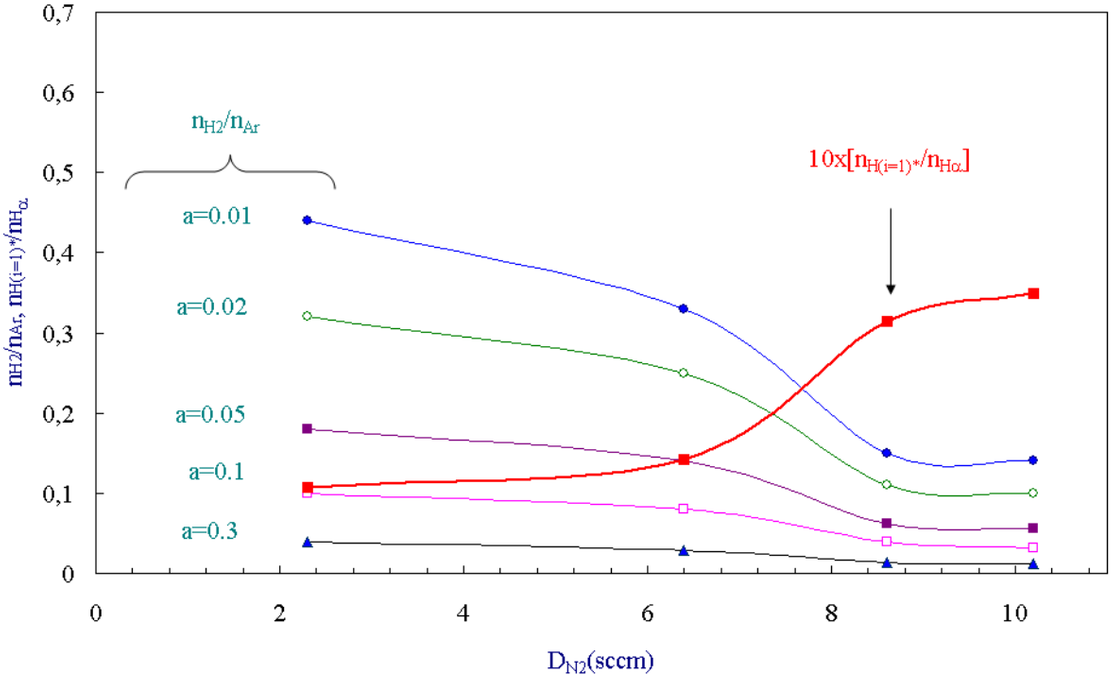

FIG.9. *$nH(i=1)/nH\alpha$ and nH_2/nAr (for different values of a) versus nitrogen gas flow rate, when $D(Ar\text{-}5\%SiH_4)$=20sccm, at 0.53mbar, 400V and 13mA.*

In the following part, we still consider the previous results shown on Figure 4. As previously written, when the nitrogen gas flow rate increases and the argon-silane gas flow rate decreases, the wings (larger broadened parts) of Hα decreases and a low components appears in the middle of the emission line which has a maximum at a nitrogen gas flow rate of 5sccm. This low energy component may be hidden by the broadened Hα spectral line observed when no nitrogen is added in gas mixture. It could be due to slow desorbed hydrogen atoms or SiH_x radicals from the reactor wall which are excited or dissociated by electron impact within the plasma. The desorbed hydrogenated species concentration decreases with decreasing Ar-5%SiH_4 concentration. According to literature hydrogen is very easily adsorbed by the surfaces of the metal, mainly in atomic form.[29] Also, it has been observed that H atoms react by etching the deposit film restoring Si-H bonds in silane plasma.[31]

Another explanation for this low energy component could be the dissociative excitation of NH_x radicals by electron impact producing slow excited H atoms. $NH_{x>1}$ species can be

produced in the gas phase or by heterogeneous reactions of NH radicals with adsorbed H atoms on the cathode or reactor wall.[32-34] J. Kurawaki et al [35] have studied the translational energy distribution (TED) of H(n=3, 4) resulting of the NH_3 dissociation process by electron impact. They found 5 components of energy ranging from 1 to 12eV. The first one at 1eV is observed at an electron energy threshold of 22.5 eV. Fast H(2s) or H(2p) atoms corresponding to this low translational energy also have been detected at lower energy thresholds 17.8eV and 16.1 to 14.7eV, respectively. Hydrogen Doppler profiles with the half widths in the range from 0.3 to 0.4 eV and from 3 to 4eV have also been detected in an Ar-NH_3 hollow cathode glow discharge. Authors explain them by the dissociative excitation and dissociative ionization of ammonia during collisions with electrons of the discharge.[36]

These different mechanisms could contribute to the formation of the low energy peak in Hα.

IV. CONCLUSION

Large broadenings of Hα and Hβ Balmer lines are observed in the Ar-5%SiH_4-N_2 DC glow discharge. These broadening results of the Doppler effect and the translational H atom energy distribution is composed of three main components observed at about 0.9 (+/-0.7)eV, 12(+/-3)eV, 62(+/-6)eV and 1.15(+/-1)eV, 26.89(+/-6)eV and 115.5(+/-12)eV for Hα and Hβ, respectively. We have shown that both low energy components result of dissociative excitation processes of H_2 by electron impact producing excited hydrogen atoms. The larger energy component observed at 62(+/-6)eV on Hα or 115(+/-12)eV for Hβ could be due to the dissociative recombination of ions in the cathode fall or to back-scattered fast H atoms on the cathode surface.

The large amount of hydrogen produced in the discharge is probably due to the effect of the wall desorption and to the recirculation of the gas within the reactor.

A low energy component is observed when the silane and nitrogen concentration decreases and increases, respectively. This component could be due to excited H atoms produced by electron impact on desorbed H atoms, SiH_x or NH_x radicals produced by etching or by reactions within the gas volume or on the reactor wall.

This work performed in hydrogen gas mixtures on broadened hydrogen Balmer line, confirms the interest of the Balmer line shapes to study the translational energy distribution of H atoms for investigations on reactive processes and on the dynamic of the plasma. It points out the role of the gas recirculation and of the reactor wall or the one of electrode surfaces in the plasma chemistry.

References .

[1] A.C. Adams, *Solid State Technol.* **26** 135 (1983).

[2] R.Aschwanden, R. Köthemann, C. Albert, M. Golla, C. Meier, *Thin SolidFilms*. **736** 138887 (2021) 6pp.

[3] Soni Prayogi, Yoyok Cahyono, Darminto, *Journal of Physics: Conference Series.* **1951** 012015 (2021). doi:10.1088/1742-6596/1951/1/012015.

[4] Shengzhi Xu, Xiaodan Zhang, Yang Li, Shaozhen Xiong, Xinhua Geng, Ying Zhao, *Thin Solid Films.* **520** 694–696 (2011).

[5] L.C. Hu, C.J. Wang, Y.W. Lin, T.C. Wei, C.C. Lee, J.Y. Chang, I.C. Chen, Y. Kawai, T.T. Lia, *ECS Journal of Solid State Science and Technology*. **4** 7 213-219 (2015).

[6] Wang Zhao-Kui, Lin Kui-Xun, Lin Xuan-Ying, Qiu Gui-Ming, Zhu Zu-Song, *Chinese Phys. Lett.* **22** 904 (2005).

[7] S. Nunomuraa, M. Kondo, *Appl. Phys. Lett.* **93** 231502 (2008) 3pp.

[8] P. Horvath, K. Rozsa, A. Gallagher, *J. Appl. Phys.* **96** 12 7660-7664 (2004).

[9] N.M. Sisovic, G.L. Majstorovic, N. Konjević, *AIP Conference Proceedings*. **1058** 143 (2008).

[10] N. Konjević, M. Ivković, N. Sakan, *Spectrochimica Acta Part B* **76** 16–26 (2012).

[11] M.R. Gemišić Adamov, B.M. Obradivić, M.M. Kuraica, N. Konjević, *IEEE Trans on plasma Sci*. **31** 444-454 (2003).

[12] Z.L. Petrović, M. Jelenković, A.V. Phelps, *Phys. Rev. Letters*. **68** 325-328 (1992).

[13] J. Perrin, J.P.M. Schmitt, *Chem. Phys. Letters.* **112** 69-73 (1984).

[14] T. Ogawa, M. Higo, *Chem. Phys.* **52** 55-64 (1980).

[15] C. Barbeau, J. Jolly, *J. Phys. D : appl. Phys.* **23** 1168-1174 (1990).

[16] E. Tatarova, F.M. Dias, N. Puač, C.M. Ferreira, *Plasma Sources Sci. Technol.* **16** S52–S56 (2007).

[17] K. Ito, N. Oda, Y. Hatano, T. Tsljboi, *Chem. Phys.* **21** 203-210 (1977).

[18] W.L. Wiese, "Plasma Diagnostic Techniques" Ed R.H. Huddleston and S.L. Leonard 265-315 Academic Press. Inc. New york, N.Y (1965).

[19] J.B. Boffard, B. Chiaro, T. Weber, C.C. Lin, *Atomic Data and Nuclear Data Tables*. **93** 831–863 (2007).

[20] CRC Handbook of chemistry and physics, 1st student edition, R.C. Weast Editor CRC Press, Inc, Boca Raton, Florida (1988).

[21] G. Norlén, *Physica Scripta.* **8** 249-268 (1973).

[22] E.B. Saloman, "Energy Levels and Observed Spectral Lines of Ionized Argon, Ar II through Ar XVIII.", *J. Phys. Chem. Ref. Data.* **39** 3 (2010).

[23] P. laborie, J.M. Rocard, J.A. Rees, "Electronic cross-sections and Macroscopic coeffficients 1- Hydrogen and rare gases.", Dunod Paris (1968).

[24] A.I. Strinić, G.N. Malović, Z.L. Petrović, N. Sadeghi, *Plasma Sources Sci. Technol.* **13** 333–342 (2004).

[25] J.B. Boffard, C.C. Lin, C.A.Jr. DeJoseph, *J. Phys. D: Appl. Phys.* **37** R143–R161 (2004).

[26] J. Perrin, J.P.M. Schmitt, *Chemical Physics.* **67** 167-176 (1982).

[27] H. Tawara, Y. Itikawa, H. Nishimura, M. Yoshino, "Cross sections and related data for electron collisions with hydrogen molecules and molecular ions", *J. Phys. Chem. Ref. Data*. **19** 3 617-636 (1990).

[28] R.K. Janev, D. Reiter, U. Samm, "*Collision Processes in Low Temperature Hydrogen plasmas."* Internal report (eirene.de/report_4105.pdf) and the two references therein: R.K. Janev, J.J. Smith, *Atomic Plasma-Matter Interaction for Data Fusion.* **4** 1 (1993); R.K. Janev, D. Langer, K. Evans, D.E. Post, "Elementary processes in hydrogen helium plasma Springer-Verlag Berlin-Heidelberg (1987).

[29] D.K. Otorbaev, M.C.M. van de Sanden, D.C. Schram, *Plasma Sources Sci. Technol.* **4** 293-301 (1995).

[30] R.F.G. Meulenbroeks, D.C. Schram, M.C.M. van de Sanden, J.A.M. van der Mullen, *Phys. Rev. Letters.* **76** 11 1840-1843 (1996).

[31] G. Turban, Y. Catherine, B. Grolleau, *Plasma Chem and Plasma Process*. **2** 61-80 (1982).

[32] Khin Swe Yin, Mundiyath Venugopalan, *Plasma Chemistry and Plasma Processing,* **3** 343-350 (1983).

[33] B.F. Gordiets, C.M. Ferreira, M.J. Pinheiro, A. Ricard, *Plasma Sources Sci. Technol.* **7** 379–88 (1998).

[34] J.L. Jauberteau, I. Jauberteau, J. Aubreton, *J. Phys. D: Appl. Phys*. **35** 665–674 (2002).

[35] J. Kurawaki, T. Ogawa, *Chem.phys* **86** 295-301 (1984).

[36] N.M. Šišović, N. Konjević, *Phys. Plasmas.* **15** 113501 7pp (2008).

Journal of Applied Physics

PLEASE CITE THIS ARTICLE AS DOI: 10.1063/5.0105384

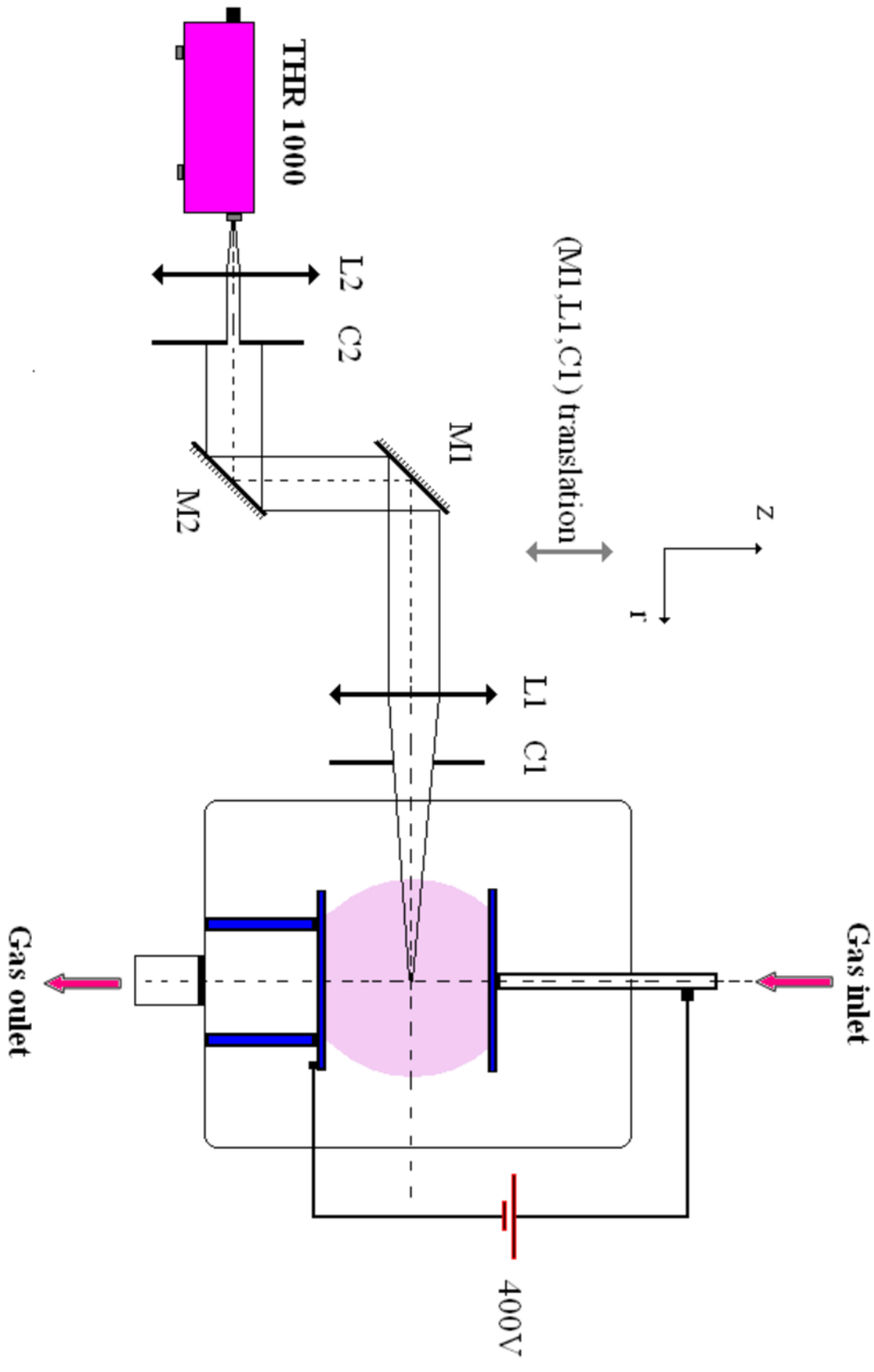

AIP Publishing

Journal of Applied Physics

ACCEPTED MANUSCRIPT

This is the author's peer reviewed, accepted manuscript. However, the online version of record will be different from this version once it has been copyedited and typeset.
PLEASE CITE THIS ARTICLE AS DOI: 10.1063/5.0105384

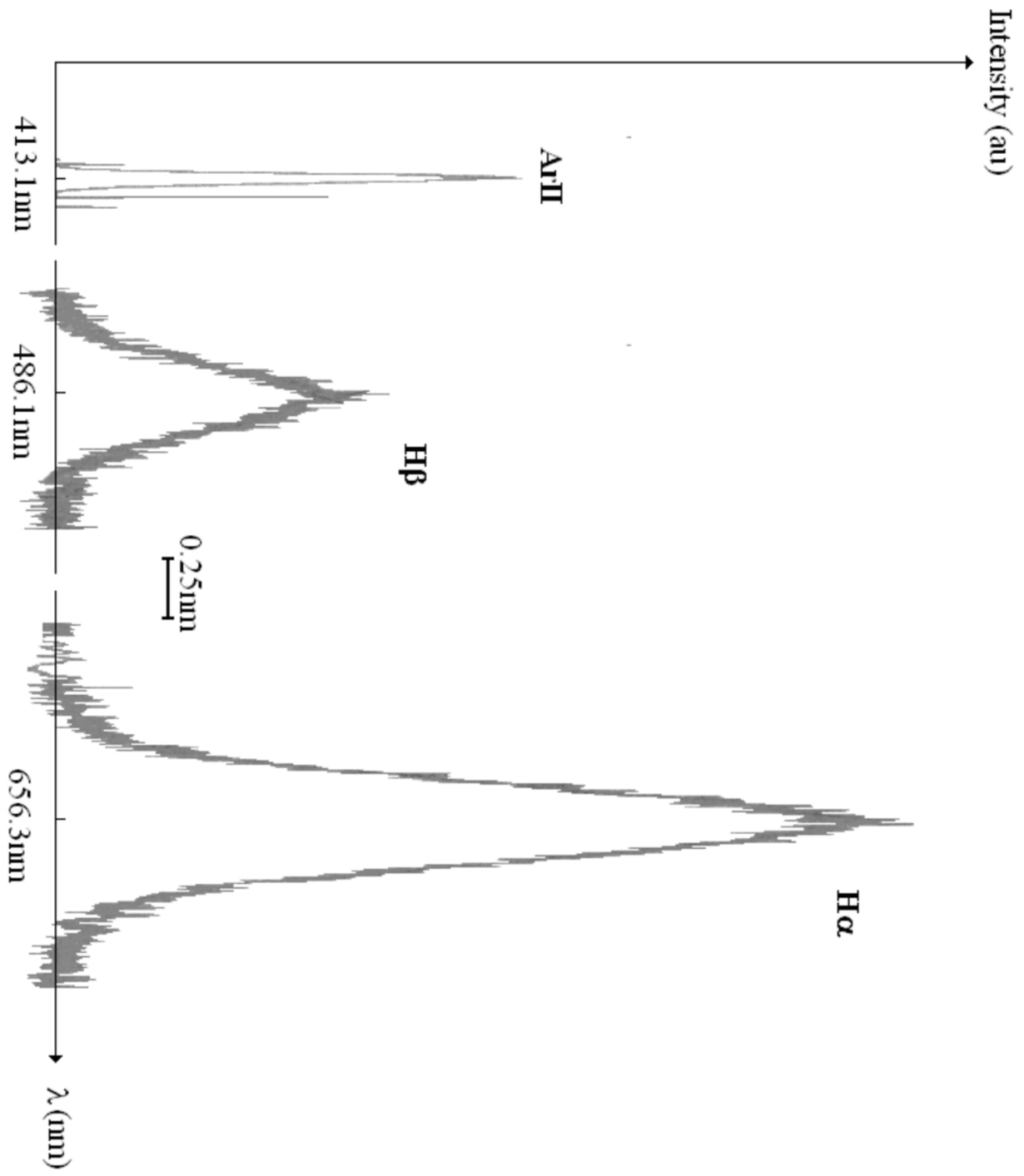

AIP Publishing

Journal of Applied Physics

ACCEPTED MANUSCRIPT

This is the author's peer reviewed, accepted manuscript. However, the online version of record will be different from this version once it has been copyedited and typeset.
PLEASE CITE THIS ARTICLE AS DOI: 10.1063/5.0105384

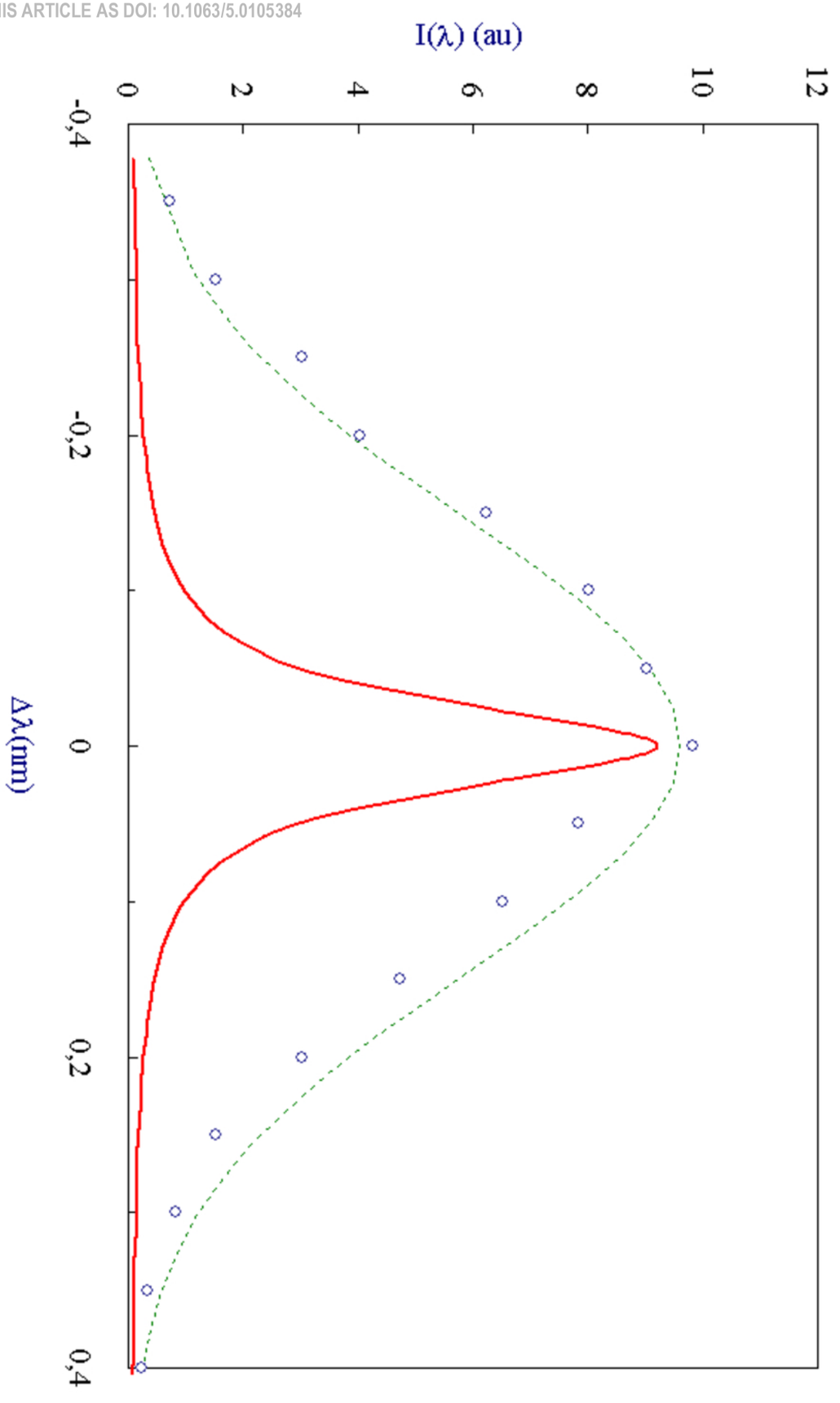

Journal of Applied Physics

AIP Publishing

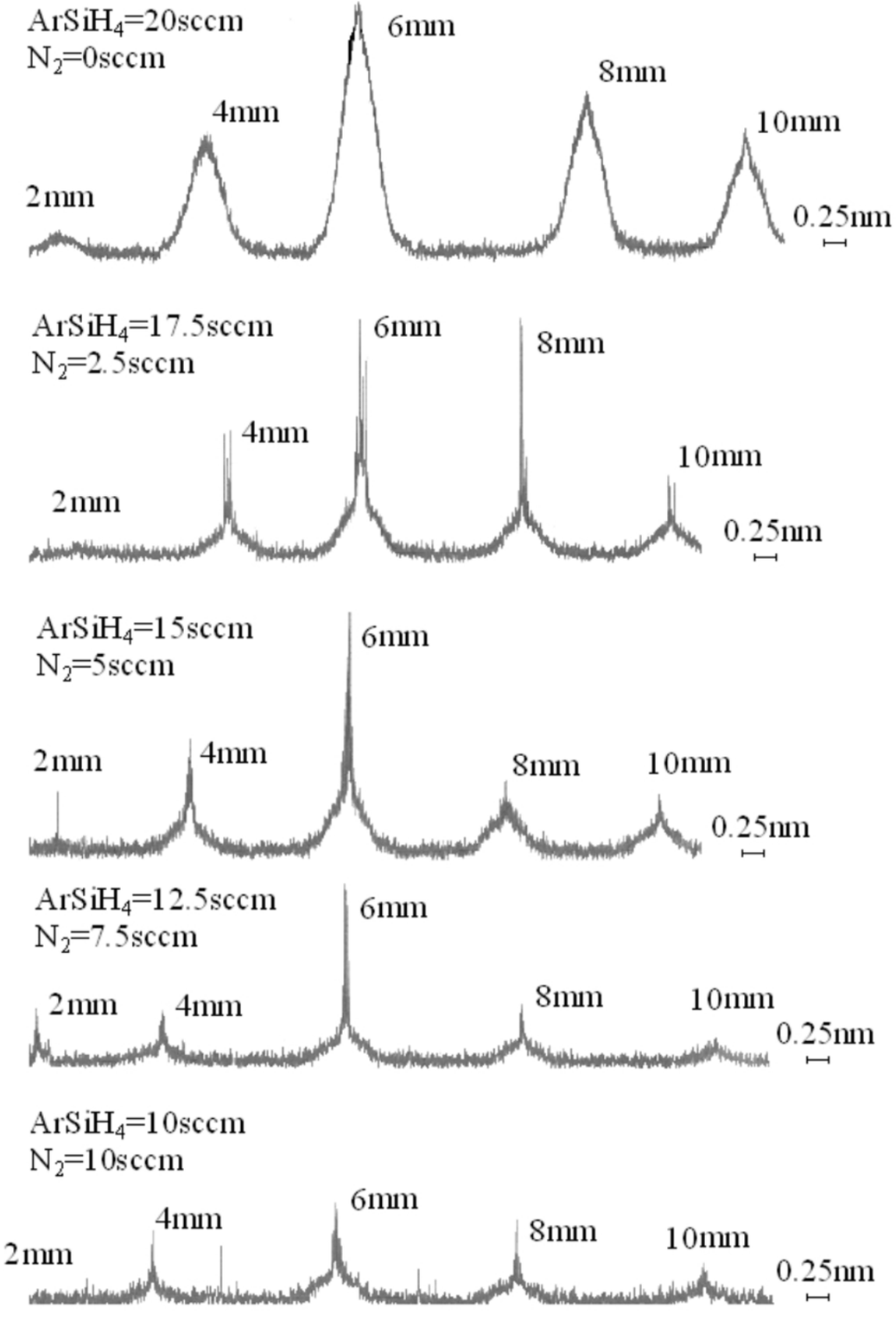

Journal of Applied Physics

PLEASE CITE THIS ARTICLE AS DOI: 10.1063/5.0105384

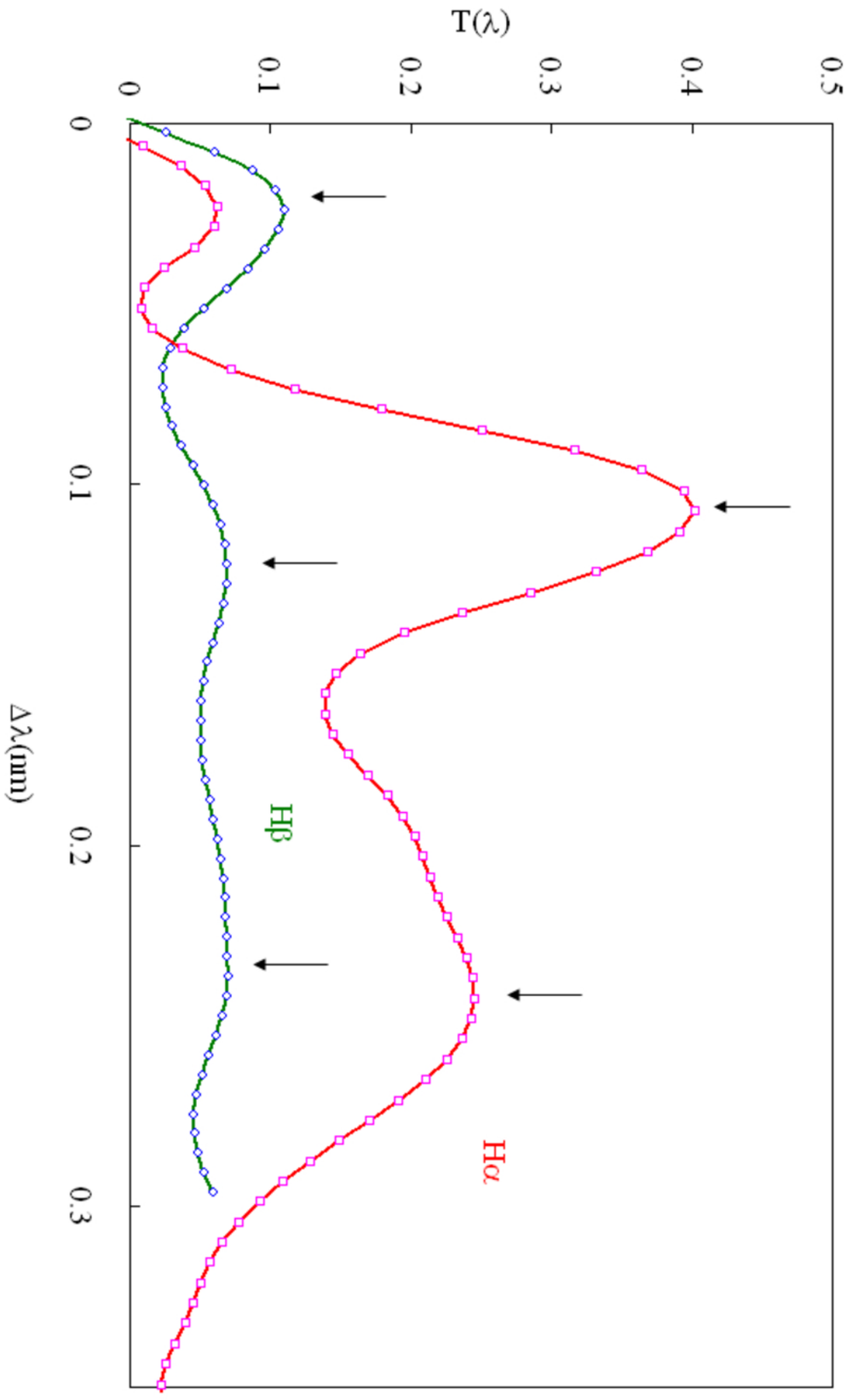

Journal of Applied Physics

PLEASE CITE THIS ARTICLE AS DOI: 10.1063/5.0105384

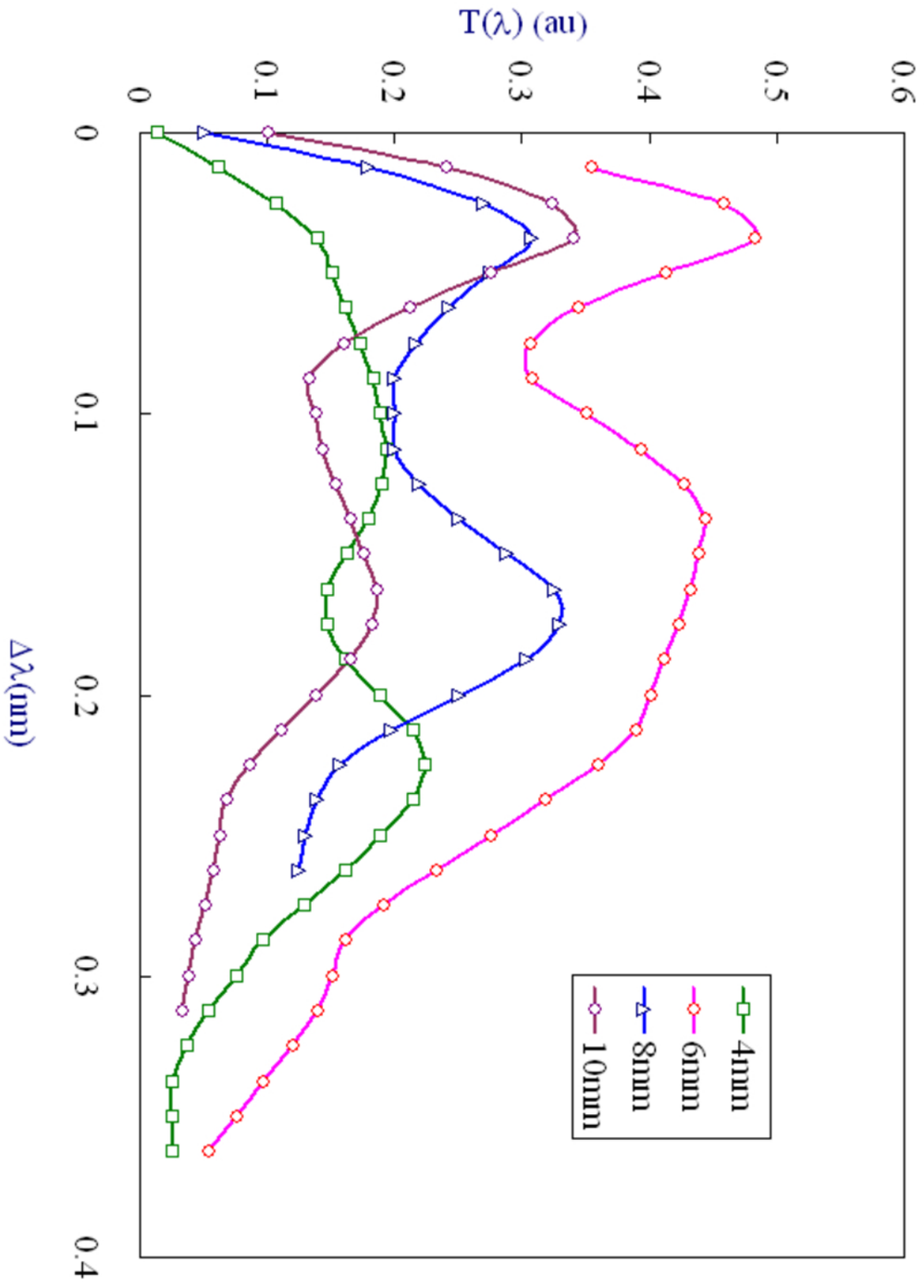

AIP Publishing

Journal of Applied Physics

ACCEPTED MANUSCRIPT

PLEASE CITE THIS ARTICLE AS DOI: 10.1063/5.0105384

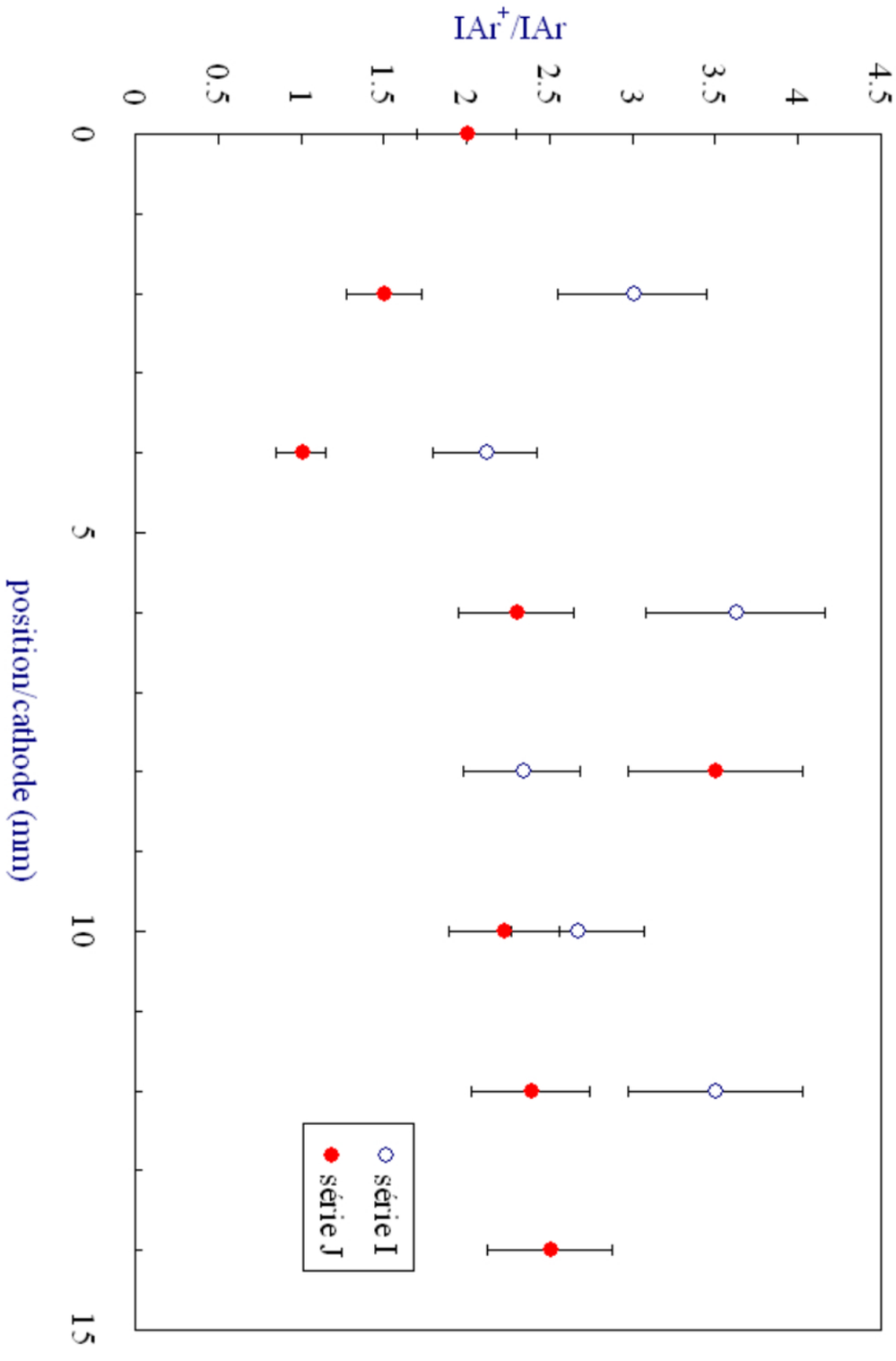

AIP Publishing

Journal of Applied Physics

ACCEPTED MANUSCRIPT

This is the author's peer reviewed, accepted manuscript. However, the online version of record will be different from this version once it has been copyedited and typeset.
PLEASE CITE THIS ARTICLE AS DOI: 10.1063/5.0105384

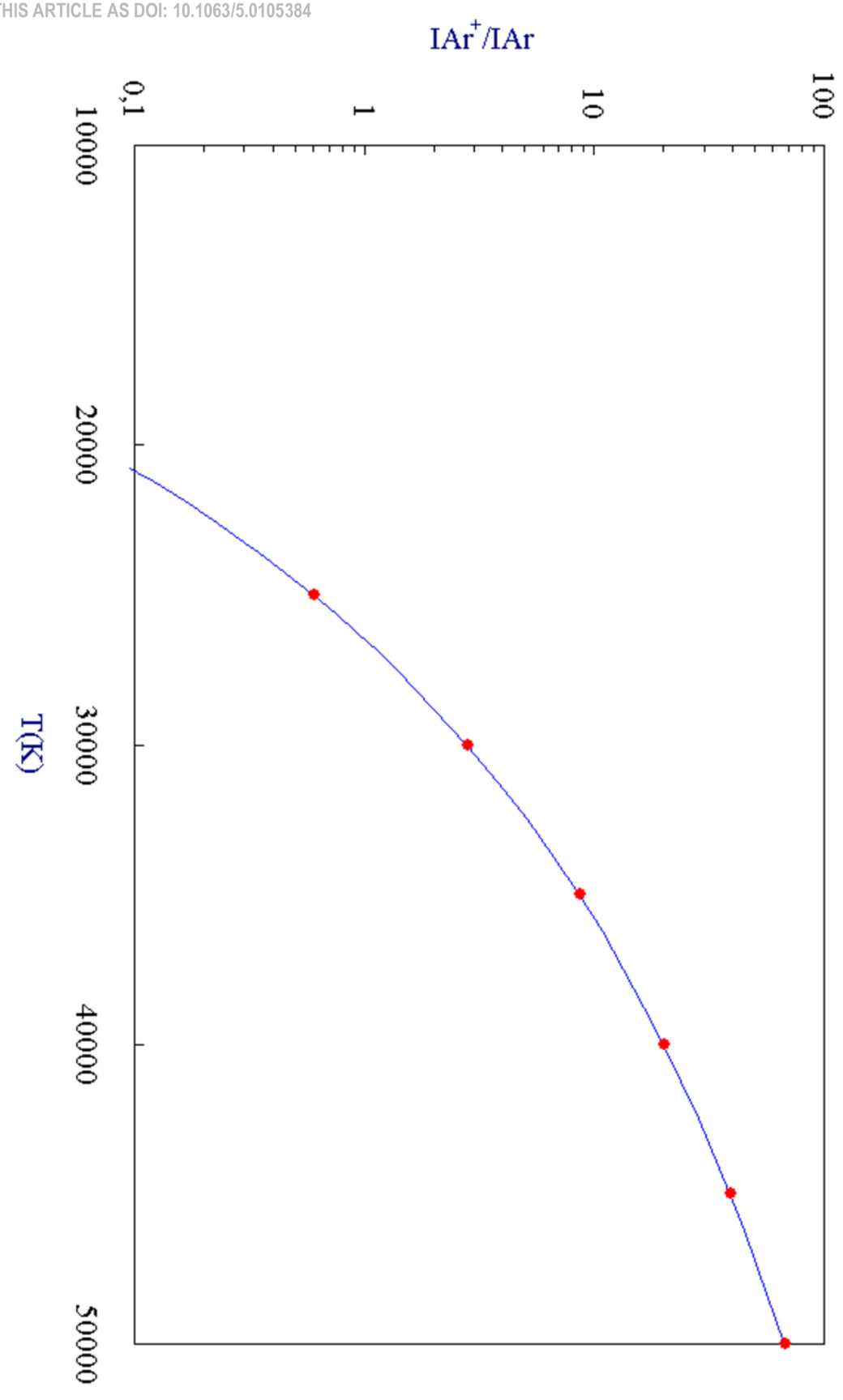

Journal of Applied Physics